December 2025

State of the Geomagnetic Field

CIRES

NATO OTAN

BGS British Geological Survey

Defence Geographic Centre

Table of Contents

DOI: 10.25923/2gcf-s393

Summary

The performance of the World Magnetic Model 2025 (WMM2025) and the World Magnetic Model – High Resolution 2025 (WMMHR2025) was evaluated by comparing their predictions for January 1, 2026, with those of a more recent model derived from data collected by the European Space Agency (ESA) Swarm satellites up to October 2025. For all magnetic field components, the global root-mean-square errors of both models increased by less than 1% over the past year and remained well below the limits specified for the WMM. Their predicted secular variation closely matched observations from ground-based observatories and Swarm-based geomagnetic virtual observatories, indicating that nonlinear changes in Earth's magnetic field remained small.

Since January 1, 2025, the north and south magnetic dip poles have moved at average speeds of 36 km/yr and 9 km/yr, respectively, with no significant change in direction—resulting in only minor adjustments in the WMM blackout zones where compass accuracy is strongly degraded. The South Atlantic Anomaly, the region of lowest geomagnetic field intensity, continued to deepen by approximately 30 nanoteslas (nT) at Earth's surface and to migrate westward by about 20 km. Over the past two years, several strong to severe geomagnetic storms as well as one extreme storm caused significant but temporary impacts on WMM performance, such as declination deviations exceeding 15 degrees at high geomagnetic latitudes.

Introduction

The World Magnetic Model (WMM) and World Magnetic Model – High Resolution (WMMHR) are spherical harmonic models of the Earth's main magnetic field and its slow temporal change. They are jointly developed by the National Centers for Environmental Information (NCEI) and the British Geological Survey (BGS) and are joint products of the United States' National Geospatial-Intelligence Agency (NGA) and the United Kingdom's Defence Geographic Centre (DGC). The WMM is the standard model used by the U.S. and U.K. governments as well as international organizations (e.g., the North Atlantic Treaty Organization and the International Hydrographic Organization) for navigation, attitude and heading referencing systems that rely on the geomagnetic field. It is also widely used in navigation and heading systems developed by organizations unaffiliated with national governments.

The main geomagnetic field is constantly changing due to convective flows of and wave motions within the Earth's liquid outer core. Because this system is essentially chaotic on longer timescales, these changes cannot be fully predicted, and the accuracy of the WMM and WMMHR gradually decreases over time. As a result, the models must be updated regularly, typically every five years.

This report reviews the performance of the latest WMM and WMMHR, released in December 2024 and referred to as WMM2025 and WMMHR2025. It also verifies that they continue to meet specification MIL-PRF-89500B (U.S. Department of Defense, 2019) as of January 1, 2026 (hereafter 2026.0; the same convention applies to other years), and provides an assessment of their secular variation after one year. This is the first such assessment of WMM2025 and WMMHR2025.

In addition, this report reviews the five-year performance of the previous WMM, released in December 2019 and referred to as WMM2020. The most recent assessment of WMM2020 was conducted in December 2023 (NCEI & BGS, 2023).

This report also describes notable changes in the Earth's main magnetic field since WMM2025 and WMMHR2025's release, including continued magnetic pole drift and the further deepening of the South Atlantic Anomaly in the geomagnetic field intensity. A separate section summarizes solar cycle progression and estimates the effects on WMM performance during magnetic storms.

WMM and WMMHR Performance: Model Errors at 2026.0

The performance of WMM2025 and WMMHR2025 was assessed at epoch 2026.0 by comparison with a more recent model derived from satellite magnetometer data. These data were collected by the European Space Agency (ESA) Swarm tri-satellite constellation from December 2013 through October 2025 (see the Appendix for more information on the Swarm model).

The WMM and WMMHR global root-mean-square errors (RMSE) for each component were calculated by adding in quadrature the omission error—associated with magnetic fields not represented in the WMM (e.g., crustal and disturbance fields)—and the commission error, which includes both the modeling error and the secular variation forecasting error. A full description of the WMM and WMMHR RMSE estimation methodology is provided in the WMM2025 technical report (WMM2025-TR; Chulliat et al., 2025). Regions where the horizontal component is smaller than 2000 nT (so-called Blackout Zones) were excluded from the declination and grid variation error calculations.

Table 1 updates information previously provided in Table 16 of the WMM2025-TR. The global RMSE for each magnetic field component was calculated at epoch 2026.0 using the Swarm-based model described above. For all components, the errors at 2026.0 for both models (rows 3 and 6) remain well below the maximum errors allowed by the WMM military specification (row 1) and the WMM error model (rows 9 and 10), which is based on estimated average errors over the five-year cycle and accounts for the geometrical relationships between components, as well as the fact that declination approaches infinity near the magnetic poles. This result is expected, as 2026.0 is only one year into the 2025–2030 WMM cycle. Additionally, a retrospective analysis of WMM2020 errors at 2025.0 (row 8) confirms that errors remained well below specification at the end of the previous cycle, consistent with the findings of the WMM2020 performance assessment conducted in late 2023 (NCEI & BGS, 2023).

Table 1: Estimated WMM2025 and WMMHR2025 global RMSEs at epochs 2025.0, 2026.0 and 2030.0, compared to the maximum global RMSEs permitted by the WMM military specification. H denotes horizontal intensity, F total intensity, I inclination angle, D declination angle, GV_N grid variation north and GV_S grid variation south. The 2030.0 values represent forecast errors based on the average error accumulated during previous five-year WMM cycles. Retrospective WMM2020 global RMSEs are provided in row 8, and WMM error model values (valid for the full 2025–2030 cycle) are provided in the last two rows. In the formulas for the declination error model, H refers to the horizontal intensity at the location where the model is evaluated. Full descriptions of the field components, the WMM uncertainty estimation methodology and the WMM error model are provided in the WMM2025-TR.

Row	Description	H (nT)	F (nT)	I (°)	D (°)	GV_N (°)	GV_S (°)
1	Military Specification MIL-W-89500B	200	280	1.00	1.00	1.00	1.00
2	Error at 2025.0 – WMM2025	130	124	0.18	0.36	0.70	0.70
3	Error at 2026.0 – WMM2025	130	125	0.18	0.36	0.70	0.70
4	Error at 2030.0 (forecast) – WMM2025	138	138	0.22	0.40	0.81	0.71
5	Error at 2025.0 – WMMHR2025	131	116	0.18	0.36	0.67	0.67
6	Error at 2026.0 – WMMHR2025	131	116	0.18	0.36	0.67	0.67
7	Error at 2030.0 (forecast) – WMMHR2025	139	131	0.22	0.40	0.77	0.68
8	Error at 2025.0 – WMM2020	139	136	0.22	0.39	0.74	0.71
9	Error Model – WMM2025	133	138	0.20	$\delta D = \sqrt{(0.26)^2 + 5417/H^2}$		
10	Error Model – WMMHR2025	130	134	0.19	$\delta D = \sqrt{(0.25)^2 + 5205/H^2}$		

As shown in Table 1, grid variation north (GV_N) exhibits the largest expected relative increase in its RMSE over the WMM cycle. GV_N is defined as the difference between magnetic declination and longitude above 55°N latitude, and its error is equal to the declination error in that region. GV_N has the largest error because (a) the declination omission error at high latitudes is larger than at lower latitudes due to more intense disturbance magnetic fields, and (b) the geomagnetic secular variation is greatest for declination in the northern polar cap as a result of the rapid drift of the north magnetic pole (see the "Magnetic Poles" section below). Figure 1 shows how the GV_N RMSE evolved over the current and previous five WMM cycles. The error was minimal at the beginning of each cycle and increased until a new model was released, reflecting the growth in secular variation forecasting error over time (hence the characteristic "sawtooth" pattern). Among the five past cycles shown, errors were smallest during the 2020–2025 cycle. It is too early in the current cycle to detect any noticeable increase in error for either WMM or WMMHR, or to make any prediction about how the error will evolve between now and 2030.

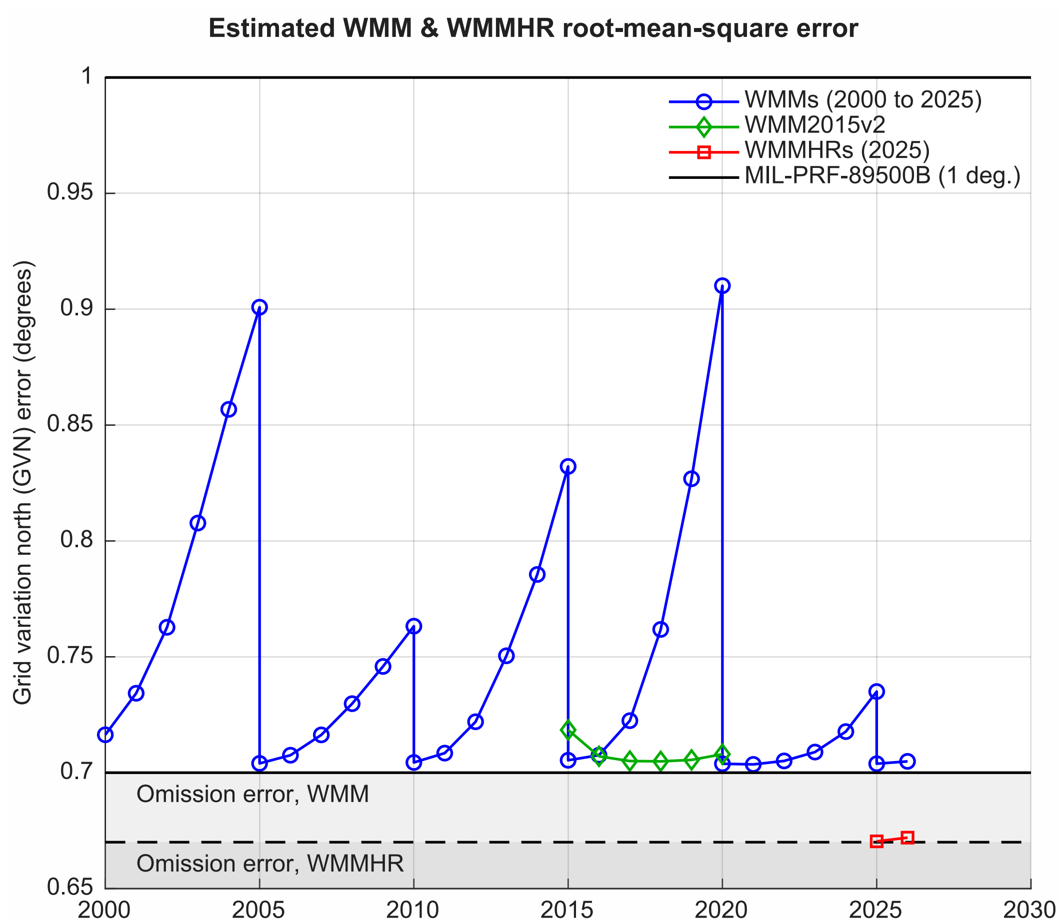

Figure 1: WMM and WMMHR global RMSE for the GV_N component from 2000 to 2026. Errors for seven successive WMMs are shown: WMM2000, WMM2005, WMM2010, WMM2015, WMM2015v2, WMM2020 and WMM2025. WMM2015v2 was an out-of-cycle update released in late 2018 in case WMM2015 breached specification before the end of its cycle (The specification was revised in 2019 with the introduction of so-called blackout zones; these zones are no longer considered in WMM error calculations, and past values have been recalculated accordingly). The first released WMMHR, WMMHR2025, is also shown, with its omission error (darker grey) slightly lower than that of the WMM due to its higher spatial resolution.

WMM and WMMHR Performance: Secular Variation Assessment

The performance of WMM2020 and initial year of WMM2025 and WMMHR2025 secular variation (SV) were assessed by comparison to subsequent independent SV observations from ground geomagnetic observatories and geomagnetic virtual observatories (GVO) from the ESA Swarm mission (Hammer et al., 2021). The method for processing each data type from 2020 through 2025 and calculating the RMSE between predicted and observed SV are described in the Appendix.

It should be noted that as SV is calculated here as annual differences of monthly means, SV data lag the most recent observations by six months; additionally, while Swarm data are delivered within four days of measurement, ground observatories may deliver their data anywhere between real-time and a lag of several years, so fewer data are typically available the closer to the present date.

The difference between the SV predictions for WMM2025 and WMMHR2025 are negligible in the context of this analysis, although SV of spherical harmonic degrees 13 to 15 are additionally included in WMMHR2025, as well as the coefficient values for degrees 1 to 12 being given to higher precision than for WMM2025.

The RMSEs between predicted and observed SV are summarised in Table 2 and can be seen to grow through the lifetime of WMM2020, as expected. Generally, they are small throughout the model's validity period and indicate good performance of the WMM2020 SV prediction globally. The discrepancy can be seen to be slightly larger in the northern polar region than in the southern, but the greatest discrepancies can be seen in middle latitudes, depicted for GVOs in Figure 2. Figure 2 shows that the SV departed most significantly from a linear trend during 2020 to 2025 in the South Atlantic, and an area from Central to Southeast Asia. These locations have seen significant secular acceleration (SA), as demonstrated in Figure 4, where timeseries of SV at selected observatories can be seen alongside successive WMM predictions.

Table 2: RMSEs between WMM2020 (white), WMM2025 (light green) and WMMHR2025 (darker green) predictions of secular variation and annual differences of monthly mean ground observatory and monthly geomagnetic virtual observatory data. Values are given for all available observations in a calendar year, as available in November 2025.

Ground observatories (at Earth's surface)

Year	dH (nT/yr)	dF (nT/yr)	dI (min/yr)	dD (min/yr)	dGV_N (min/yr)	dGV_S (min/yr)
2020	7	7	1	2	3	1
2021	10	10	1	2	3	2
2022	12	13	1	3	4	2
2023	12	14	2	3	3	2
2024	15	16	2	3	2	3
2025	13	8	1	2	2	3
2025 HR	13	8	1	2	2	2

Geomagnetic Virtual Observatories (at 490 km)

Year	dH (nT/yr)	dF (nT/yr)	dI (min/yr)	dD (min/yr)	dGV_N (min/yr)	dGV_S (min/yr)
2020	3	4	1	2	6	1
2021	5	6	1	2	4	1
2022	7	8	1	2	6	2
2023	10	11	2	2	5	3
2024	11	11	2	3	7	2
2025	3	3	0	1	5	1
2025 HR	3	3	0	1	5	1

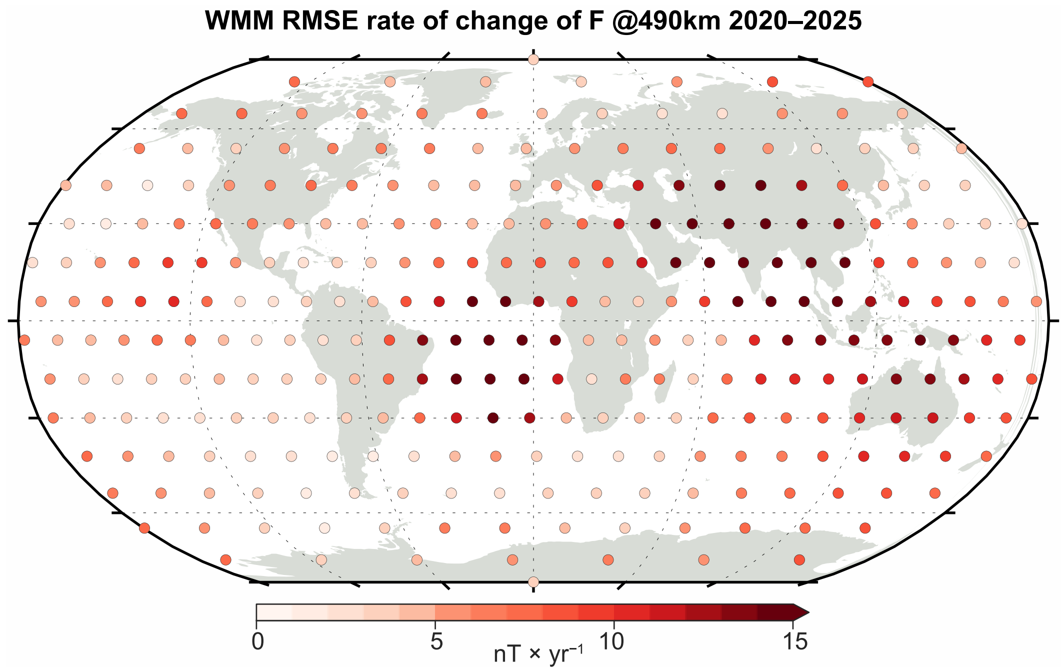

Figure 2: RMSE between prediction of WMM2020 SV of total intensity (F) and geomagnetic virtual observatory data for 2020 to 2025.

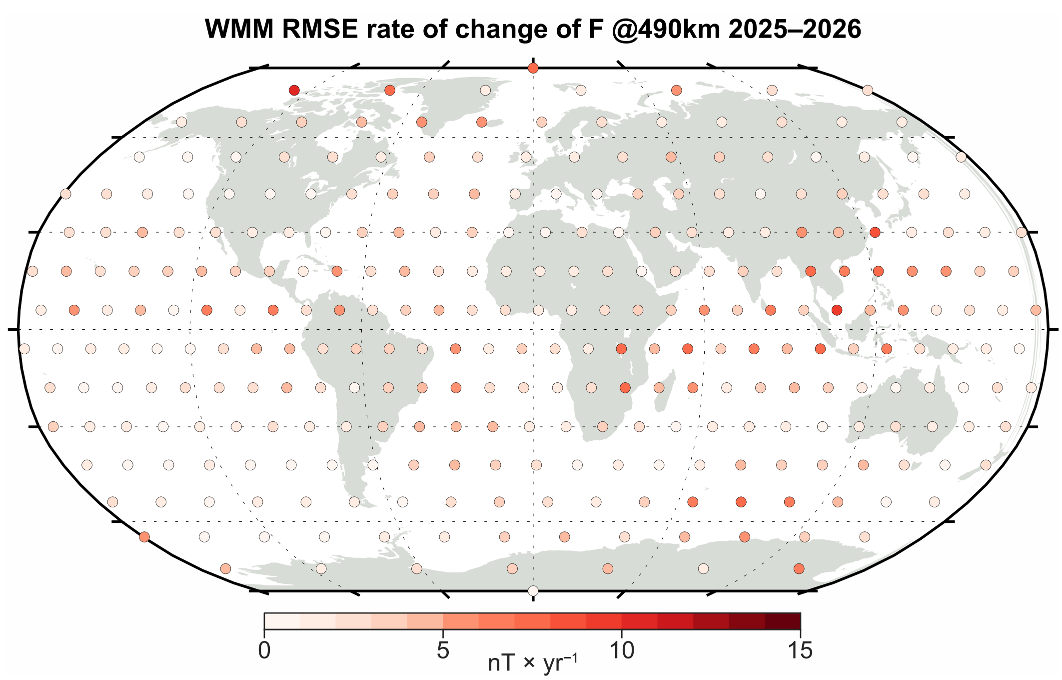

Figure 3: RMSE between prediction of WMM2025 SV of total intensity (F) and geomagnetic virtual observatory data in 2025.

The mapped RMSE values for observatories (not shown) generally show consistently higher values at high latitudes, where unmodelled external and induced field signals are present in the data to a greater extent, and also display the pattern seen at GVO altitude. The differences between observed and predicted SV of H shown in Table 2 are larger for the 2025 values of WMM2025 and WMMHR2025 than for the comparable 2020 values for WMM2020. This does not necessarily indicate a poor performance of the SV prediction in the initial year. We attribute this larger RMSE to two factors: 25% of the limited available observatory data at time of analysis in November 2025 are at high latitudes, where larger RMSE is expected due to external field influence; and 2024 and 2025 have seen significant periods of high geomagnetic activity, leading to greater scatter in the data. Though we select data for geomagnetically quiet times to mitigate this, this leaves few data points at times of frequent heightened activity, and thus the monthly means that result are less robust to scatter in the observations that remain. These initial estimates of SV prediction RMSE may reduce on reanalysis in 2026, when a greater number of data are available for 2025.

There is not a clear pattern of regional scale secular acceleration present in the RMSEs for the initial year of WMM2025 and WMMHR2025, depicted for GVOs in Figure 3, though the known regions of strong SA during 2020 to 2025 can be identified weakly. Figure 4 gives context for this early assessment of the 2025 predictions of SV at ground observatories. The new models begin very close to the observed SV, but two particular trends are visible already when viewed at an individual observatory level: a continuing period of large, approximately constant SA in the South Atlantic and over Southeast Asia; and a recent geomagnetic jerk (a rapid change in SA) as demonstrated in the Pacific and Australia in late 2023/early 2024 in Figure 4. While we cannot predict future SV with certainty, the presence of this jerk so close to the start of WMM2025, suggests that these regions may see increased discrepancy between the predicted and observed SV over the lifespan of WMM2025. As depicted in Figure 4, similar situations occurred for WMM2015 and WMM2020, and we do not anticipate issues with the prediction meeting the specification thresholds before 2030. Overall, the RMSEs observed so far for the 2025–2030 period are small, and within the expected range.

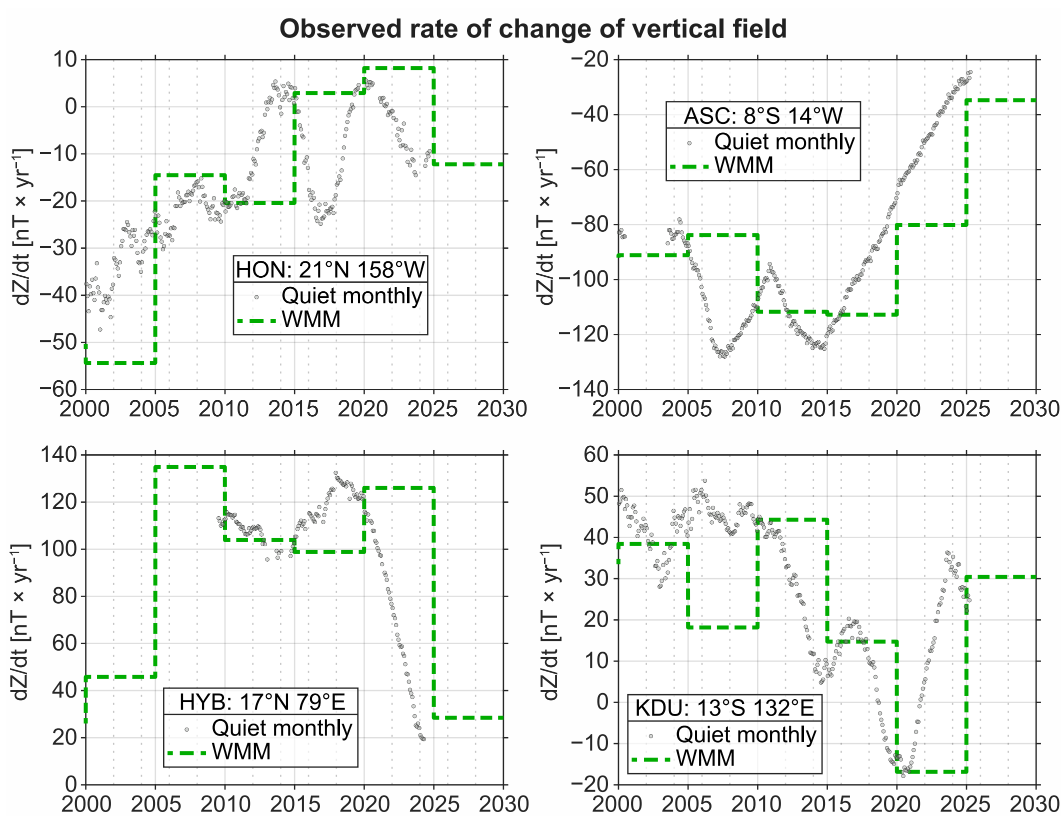

Figure 4: Observed rate of change of vertical field (Z) in nanotesla per year at (top left) Honolulu, Hawai'i, United States (HON), (top right) Ascension Island, South Atlantic (ASC), (bottom left) Hyderabad, India (HYB) and (bottom right) Kakadu, Australia (KDU). Quiet-dark monthly mean data (see Appendix) are shown as gray circles, and WMM predictions (WMM2000, WMM2005, WMM2010, WMM2015v2, WMM2020, WMM2025) are shown by the green dashed line.

Magnetic Dip Poles and Blackout Zones

Magnetic dip poles, defined as the points where the geomagnetic field is exactly vertical (i.e., perpendicular to the ellipsoid), drift over time as the main magnetic field gradually changes. WMM2025 and WMMHR2025 pole locations are available at https://www.ncei.noaa.gov/products/wandering-geomagnetic-poles and https://geomag.bgs.ac.uk/education/poles.html. Figures 5 and 6 show the pole locations at 2026.0 and at the beginning (2025.0) and end (2030.0, predicted) of the WMM2025 cycle.

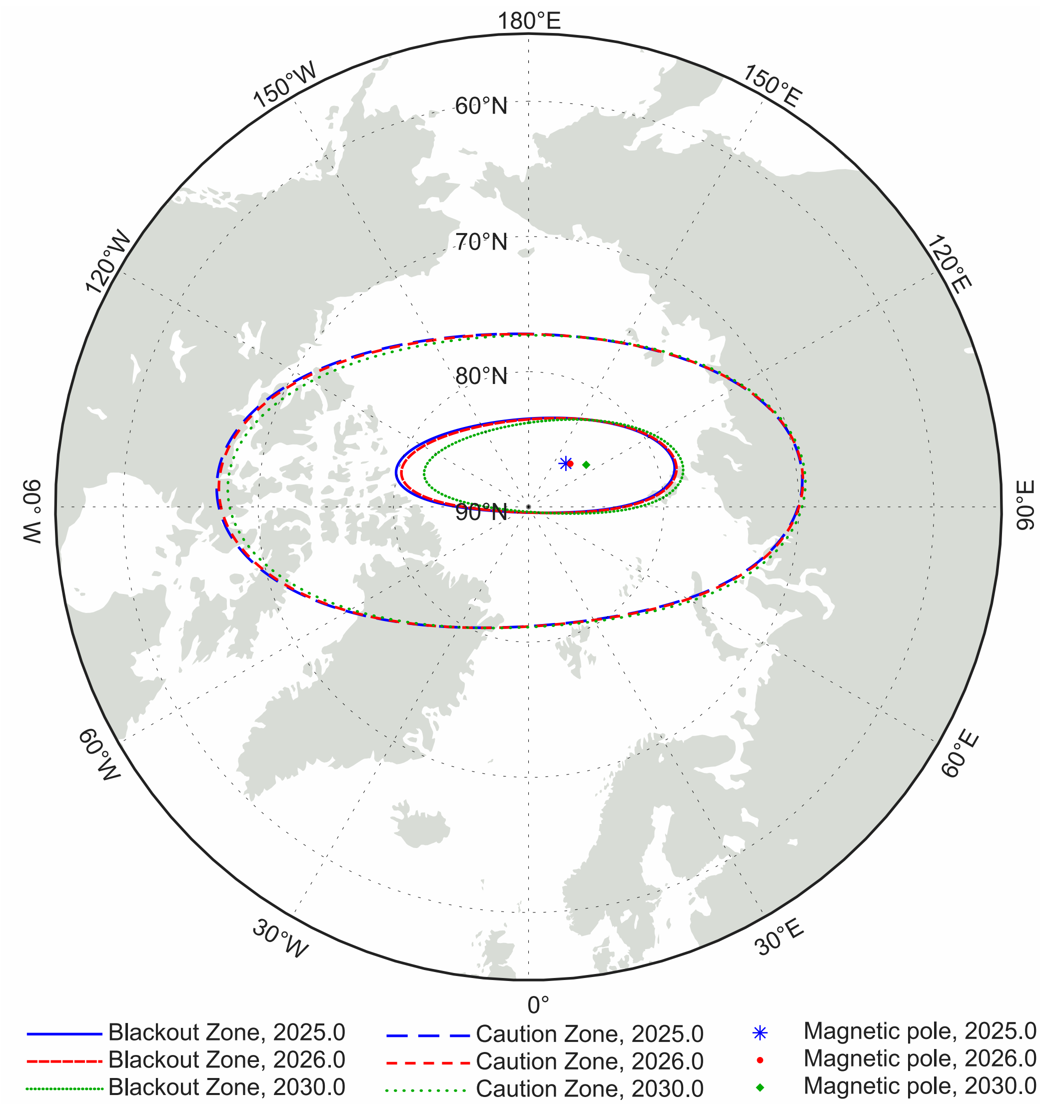

Figure 5: Successive locations of the magnetic dip pole, Blackout Zone and Caution Zone in the northern hemisphere throughout the WMM2025 five-year cycle.

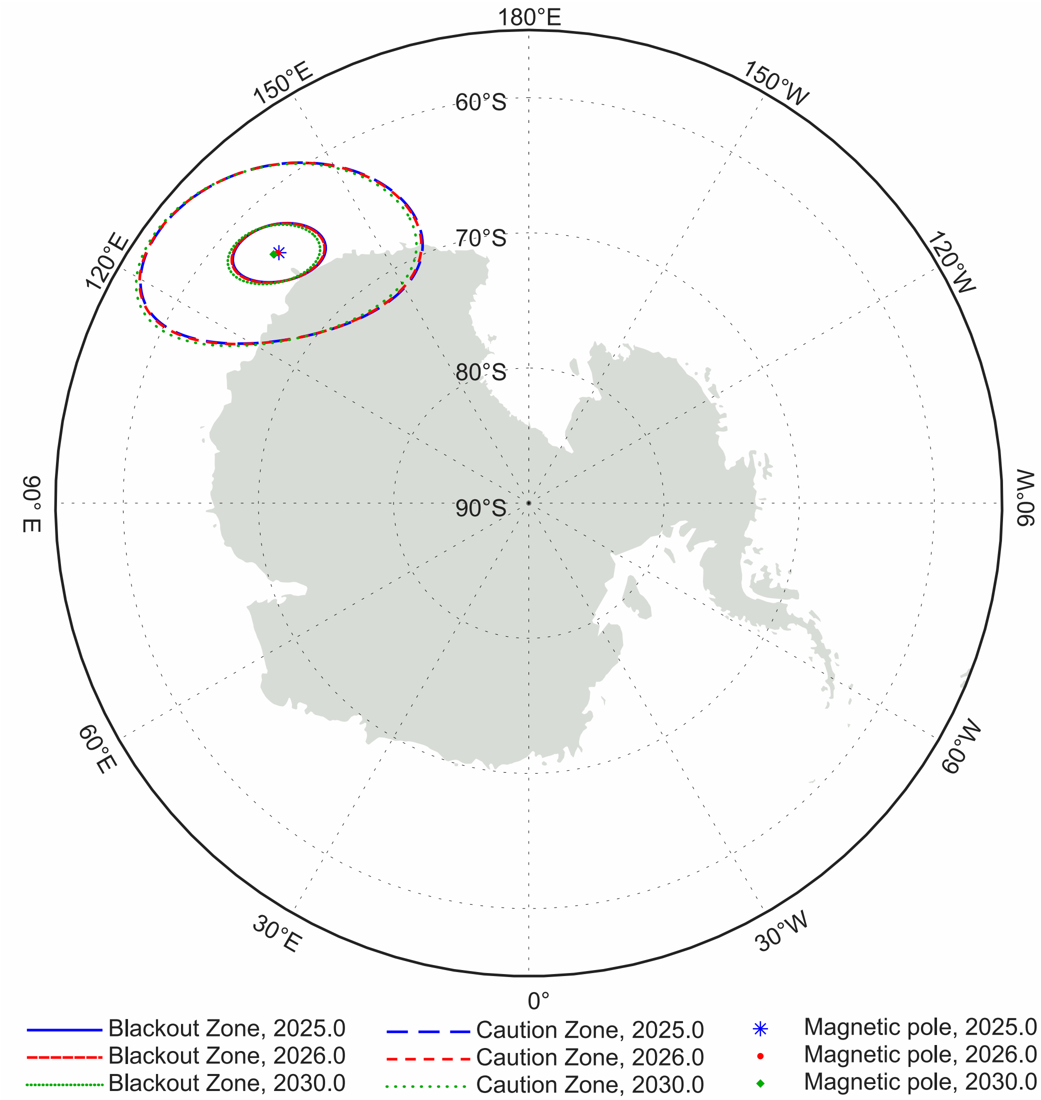

Figure 6: Successive locations of the magnetic dip pole, Blackout Zone and Caution Zone in the southern hemisphere throughout the WMM2020 five-year cycle.

Actual pole locations from 2025.0 to 2026.0 were determined using the Swarm-based model described in the Appendix. The distances between the predicted magnetic pole locations from WMM2020, WMM2025 and WMMHR2025 and the observed pole locations remained small relative to the annual movement of each pole (Table 3), demonstrating that all three models have remained highly accurate in the polar regions since their release. Distances are slightly smaller for WMMHR2025 than WMM2025, reflecting the higher spatial resolution of WMMHR's core field component. Because WMM2025 closely matches the observed positions, only WMM2025 locations are shown in Figures 5 and 6.

Table 3: Distances between the annual predicted magnetic pole locations from WMM2020, WMM2025 and WMMHR2025 and the observed magnetic pole locations in the northern and southern hemispheres.			
Epoch	**Model**	**Distance to observed pole – North (km)**	**Distance to observed pole – South (km)**
2020.0	WMM2020	0.3	1.5
2021.0	WMM2020	3.9	1.0
2022.0	WMM2020	6.2	1.5
2023.0	WMM2020	6.7	1.8
2024.0	WMM2020	7.4	3.0
2025.0	WMM2020	9.5	3.7
2025.0	WMM2025	3.6	2.2
2026.0	WMM2025	5.7	2.4
2025.0	WMMHR2025	2.3	1.2
2026.0	WMMHR2025	5.6	1.5

Between 2025 and 2026, the north magnetic dip pole was the fastest moving, with an average drift speed of 36 km/year, compared to 9 km/year for the south dip pole. The observed drift speed has remained close to the WMM2025 forecast (Figure 7), as in the previous cycle. This contrasts with 2015–2020, when a sudden acceleration of the north dip pole shortly after WMM2015's release led to differences of up to 10 km/year between forecast and observation, later corrected by the out-of-cycle WMM2015v2 update. WMM2025 and WMMHR2025 predict that the north dip pole's drift speed will gradually decrease to just above 30 km/year by the end of the decade.

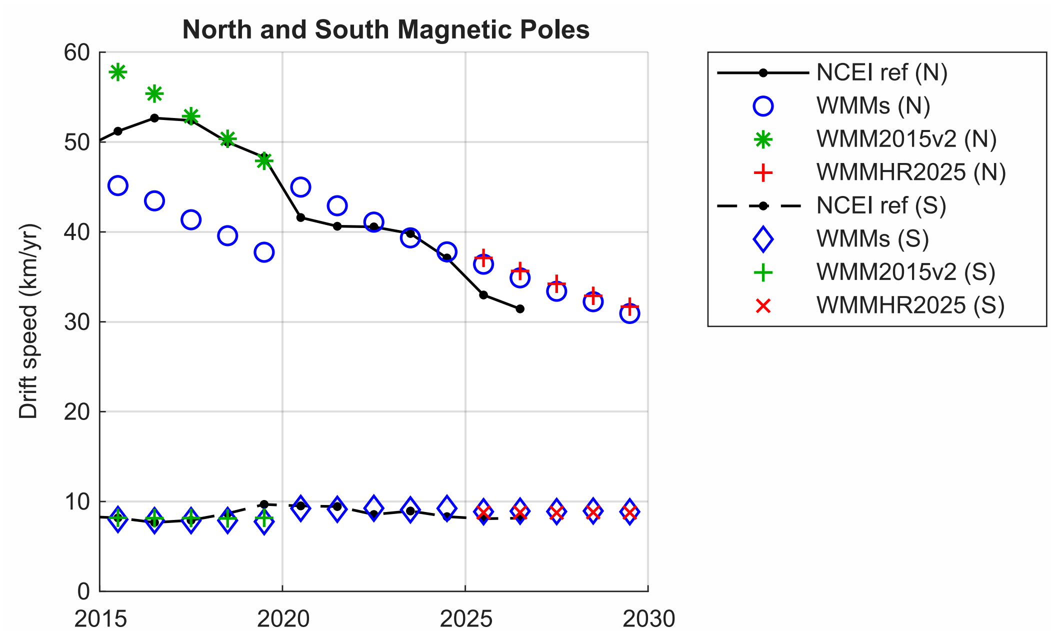

Figure 7: Drift speed of the north and south magnetic poles, as predicted by the updated Swarm-based core field model (black solid and dashed lines); WMM2015, WMM2020 and WMM2025 (blue circles and diamonds); WMM2015v2 (green stars and crosses); and WMMHR2025 (red plus signs and crosses).

As dip poles drift, WMM2020 Blackout Zones and Caution Zones slowly change over time (Figures 5 and 6). Blackout Zones are defined as regions of the World Geodetic System 1984 (WGS84) ellipsoid where the horizontal component of the magnetic field is less than 2000 nT. In Blackout Zones, WMM declination values are not accurate and compass accuracy is degraded. Caution Zones are regions where the horizontal intensity is less than 6000 nT and greater than 2000 nT. Blackout and Caution Zones are automatically updated in NCEI online calculators.

South Atlantic Anomaly

The South Atlantic Anomaly (SAA) is a region spanning the southern Atlantic and South America where the Earth's magnetic field is at its weakest. In the SAA the intensity of the field is about one-third of that near the magnetic poles. The SAA affects how closely energetic charged particles can reach the Earth, which impacts satellite radiation damage and radio propagation. Polar regions are also strongly affected by energetic charged particles, but the impacts there are less dependent on field intensity.

The SAA is deepening and moving westwards. Table 4 shows the change in the SAA from 2025.0 to 2026.0 as estimated at Earth's surface and at 500 km by WMM2025 and WMMHR2025. The area affected, as judged by the area inside the 25,000 nT contour at the Earth's surface, has increased by about 8% over this time (for both WMM and WMMHR). This contour approximates the region where radiation damage to satellites is most likely to occur.

Table 4: Monitoring the SAA intensity and location (defined as the point of minimum total field intensity, F) from 2025 to 2026 for WMM2025 and WMMHR2025.

Epoch	Altitude (km)	Minimum F (nT) WMM (WMMHR)	Latitude (°S) WMM (WMMHR)	Longitude (°W) WMM (WMMHR)
2025.0	0	22079 (22037)	−26.1 (−27.3)	299.9 (301.5)
2026.0	0	22049 (22009)	−26.1 (−27.3)	299.7 (301.5)
2025.0	500	18310 (18311)	−22.3 (−22.3)	300.6 (300.7)
2026.0	500	18287 (18287)	−22.3 (−22.3)	300.4 (300.5)

An updated analysis shows the progression of the SAA as predicted by the Swarm-based model described in the Appendix. The magnetic field strength 500 km above Earth is shown in Figure 8, with SAA regions highlighted by white contour lines. The location of the weakest magnetic field is marked by a yellow asterisk. The minimum value predicted by the latest model is 18,285 nT at –22.28° latitude and 300.44° longitude, which closely matches the WMM2025 predictions for the same date (Table 4). These results confirm that the WMM2025 predictions of SAA progression remain accurate.

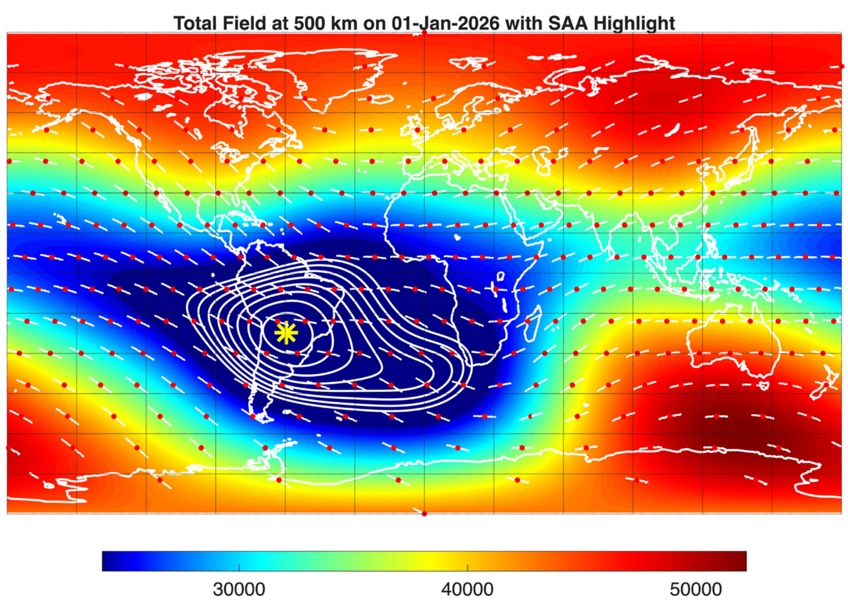

Figure 8: Magnetic field strength 500 km above Earth as predicted by the updated Swarm-based core field model for January 1, 2026. Recent trends in the strength observed from Swarm GVO data between 2020.5 and 2025.5 are overlaid. The yellow asterisk marks the location of the weakest field.

Solar Cycle Progression and Magnetic Storms

The Sun goes through an approximate 11-year cycle in activity (Figure 9), but space weather impacts can occur at any point during the cycle. As depicted in Figure 9, we have recently passed the peak of solar cycle 25 in terms of sunspot numbers but are now in the period when magnetic activity peaks (1–2 years post-sunspot number peak) and larger, more frequent geomagnetic storms are common. Space weather impacts relevant for the WMM user community are many and varied and include power outages, radio communications, satellite operations, etc. Space weather's impact on navigation is given particular consideration here due to differences between the WMM declination estimates and the actual declination during a space weather event. The magnetic field variations resulting from sources outside the Earth are considered in WMM error estimates in a root-mean-square sense. However, it is of interest to list extreme events over recent years and map the maximum declination deviations during these events as recorded on the ground by the network of observatories.

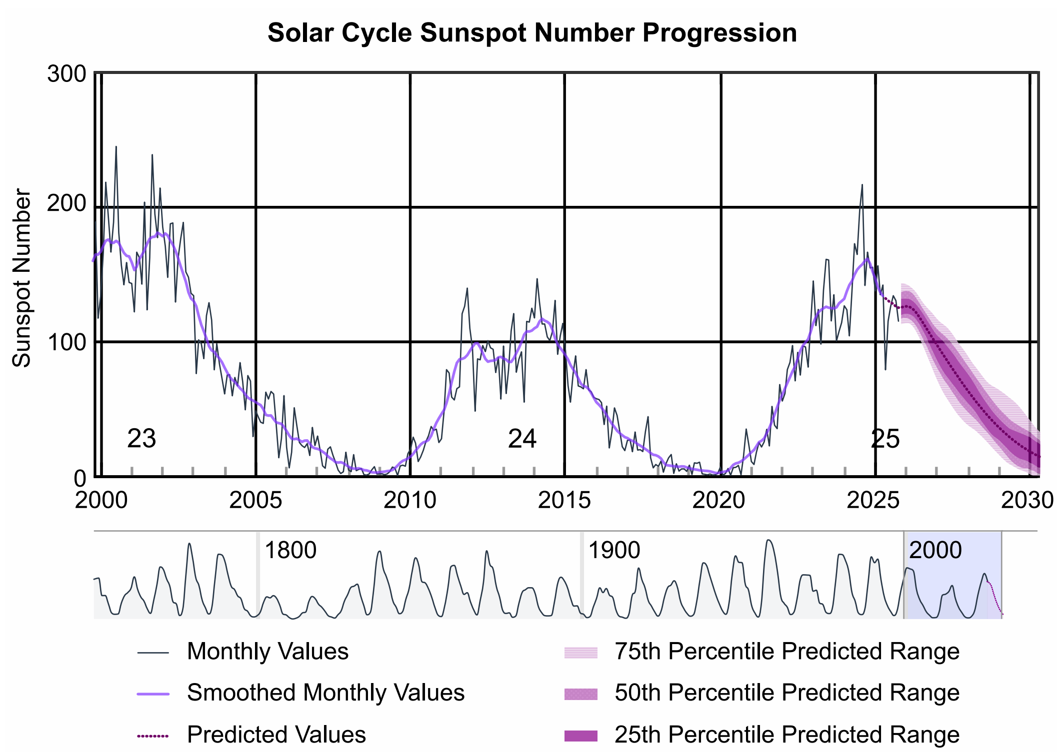

Figure 9: Observed and predicted solar cycle since 2000. The black line represents the monthly average sunspot number, and the light purple line represents a 13-month weighted, smoothed version of the monthly averaged data. The forecast for the current solar cycle is represented by the dark purple line, with its 75th percentile range as a shaded pink area. This forecast comes from the Solar Cycle Prediction Panel representing NOAA, NASA and the International Space Environmental Services (ISES). Image provided by the NOAA Space Weather Prediction Center, updating the 2019 expert panel prediction (https://www.swpc.noaa.gov/products/solar-cycle-progression).

Using the NOAA Space Weather Prediction Center method of reclassifying magnetic storms by magnetic activity index Kp into the geomagnetic (G) storm scale G1–G5, a list of the largest storms—namely G3–G5 storms—during the period of November 1, 2023, to October 31, 2025 is presented in Table 5. This period covers the current report and extends back to the end of the period included in the previous State of the Geomagnetic Field report (NCEI & BGS, 2023). As this period spans the most active portion of the solar cycle, the list of storms is considerable, and not all are discussed in detail.

Table 5: List of G3 to G5 magnetic storms from November 1, 2023, to October 31, 2025, occurring since the last State of the Geomagnetic Field report issued in December 2023. For some storms, the approximate peak or center day of extended activity is indicated. The two largest recent storms are highlighted.

Date	Max Kp	NOAA storm classification
05 Nov 2023	7+	G3
01 Dec 2023	7−	G3
24 Mar 2024	8+	G4
19 Apr 2024	7	G3
02 May 2024	7−	G3
11 (10–12) May 2024	**9**	**G5**
28 Jun 2024	8−	G4
04 Aug 2024	7	G3
12 Aug 2024	8	G4
12 Sep 2024	8	G3
17 Sep 2024	7	G3
10 (8,10) Oct 2024	**8+**	**G4**
01 Jan 2025	8	G4
16 Apr 2025	8−	G4
01 Jun 2025	8−	G4
15 Sep 2025	7−	G3
01 Oct (30 Sep, 02 Oct) 2025	7	G3
18 Oct 2025	7−	G3

Figures 10 and 11 depict the maximum absolute D deviation (see methods in the Appendix). The purpose of these figures is to illustrate an indicative worst case and global pattern rather than a real WMM error. It is "indicative" because local crustal fields are excluded, and it is "worst case" because standard errors arising from external sources are already included in the WMM error estimates. As expected, high-latitude regions experience the largest maximum D deviations during magnetic storms: up to 15.1° in Canada during the G5 storm on May 10–12, 2024, the first G5 storm seen since 2003; and up to 16.7° in Greenland during the G4 storm on October 8–10, 2024. Lower D deviation values are seen in the southern hemisphere, in part due to the limited observations available at the appropriate magnetic latitudes.

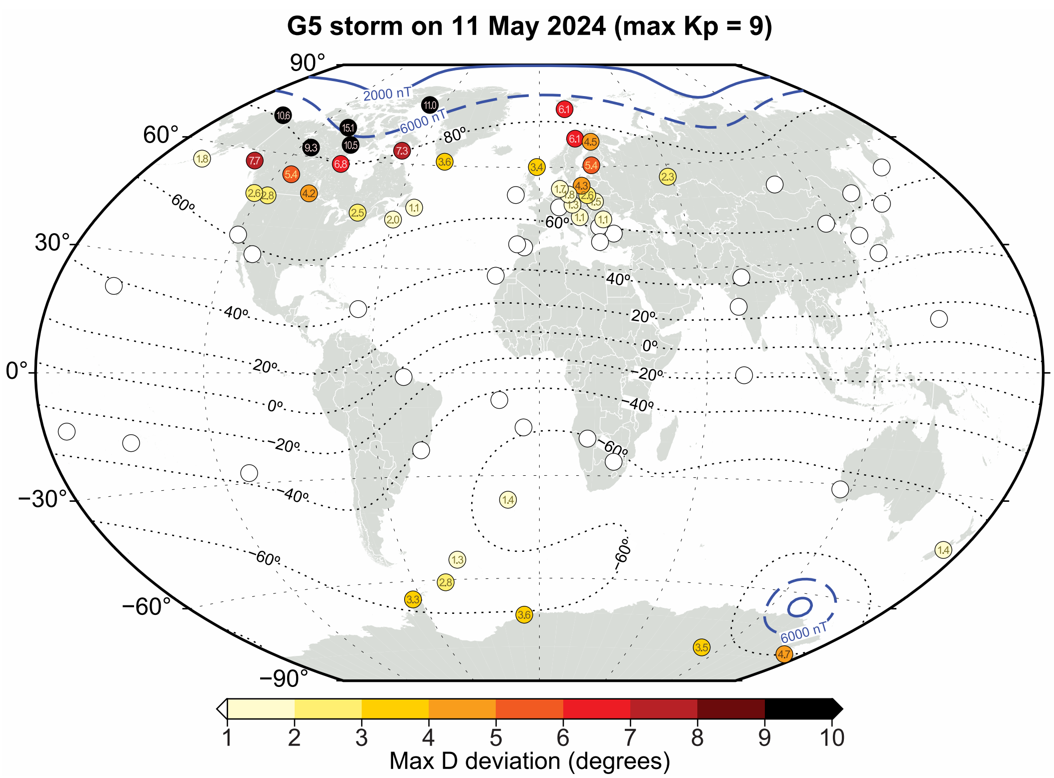

Figure 10: Indicative maximum declination deviations during the G5 storm of May 10–11, 2024, known as the Gannon storm. The white circles are observatories where the maximum deviation is less than the military specification of 1°, and black circles are those where it is over 9°. The blue solid contour indicates the horizontal field value used to mark the WMM blackout zone (2000 nT); the blue dashed contour indicates the same for the caution zone (6000 nT). The black dotted contours show the inclination of the magnetic field vector. Field values are from WMM2020.

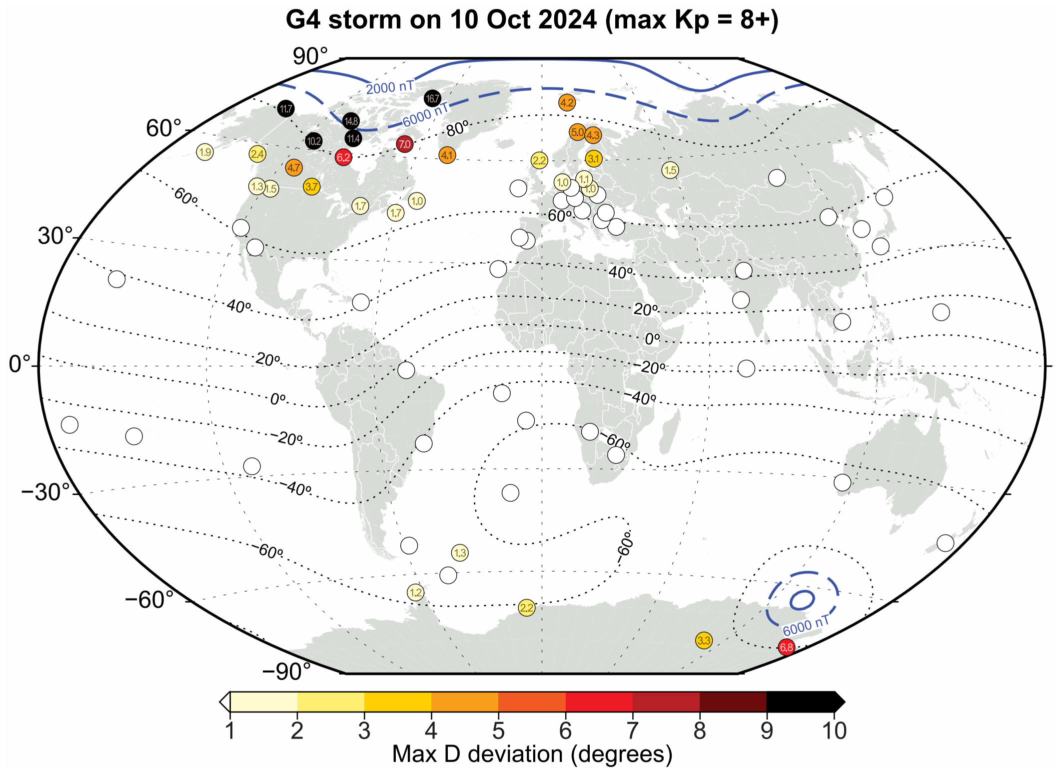

Figure 11: Indicative maximum declination deviations during the G4 storm of Oct 8–10, 2024. The white circles are observatories where the maximum deviation is less than the military specification of 1°, and black circles are those where it is over 9°. The blue solid contour indicates the horizontal field value used to mark the WMM blackout zone (2000 nT); the blue dashed contour indicates the same for the caution zone (6000 nT). The black dotted contours show the inclination of the magnetic field vector. Field values are from WMM2020.

Further large storms may be expected during the early lifespan of WMM2025 and WMMHR2025, but they should generally decline in intensity and frequency towards 2030 and the next solar minimum.

For detailed space weather services, the WMM user is referred to NOAA Space Weather Prediction Center (https://www.swpc.noaa.gov/), ESA Space Weather Service Network (https://swe.ssa.esa.int/current-space-weather) and BGS Space Weather Services (https://geomag.bgs.ac.uk/data_service/space_weather/home.html).

References

Chulliat, A., Brown, W., Nair, M., Gomez Perez, N., Young, L.-Y., Watson, C., Boneh, N., Beggan, C., Meyer, B., & Paniccia, M. (2025). The US/UK World Magnetic Model for 2025–2030: Technical report. National Centers for Environmental Information, NOAA. https://doi.org/10.25923/prbc-s316

Hammer, M. D., Cox, G. A., Brown, W. J., Beggan, C. D., & Finlay, C. C. (2021). Geomagnetic Virtual Observatories: monitoring geomagnetic secular variation with the Swarm satellites. Earth, Planets and Space, 73(1). https://doi.org/10.1186/s40623-021-01357-9

Kloss, C., Finlay, C. C., Olsen, N., Tøffner-Clausen, L., Gillet, N., & Grayver, A. (2025). CHAOS-8 geomagnetic field model (8.4). Zenodo. https://doi.org/10.5281/zenodo.17225475

Maus, S., Yin, F., Lühr, H., Manoj, C., Rother, M., Rauberg, J., Michaelis, I., Stolle, C., & Müller, R. D. (2008). Resolution of direction of oceanic magnetic lineations by the sixth-generation lithospheric magnetic field model from CHAMP satellite magnetic measurements. Geochemistry, Geophysics, Geosystems, 9(7). https://doi.org/10.1029/2008gc001949

National Centers for Environmental Information (U.S.) & British Geological Survey (2023). State of the Geomagnetic Field 2023. https://doi.org/10.25923/cww1-sc35

U.S. Department of Defense (2019). Performance specification—World Magnetic Model (WMM) (Doc. MIL-PRF-89500B). http://everyspec.com/MIL-PRF/MIL-PRF-080000-99999/MIL-PRF-89500B_56010

Swarm Reference Model

In October 2025, we developed a reference geomagnetic core field model from recent Swarm satellite data to support the evaluation of the World Magnetic Model 2020 (WMM2020), WMM2025 and the World Magnetic Model – High Resolution 2025 (WMMHR2025). We used Swarm A and B vector magnetic data from December 2013 until mid-October 2025. The Swarm data were preprocessed by selecting measurements collected between midnight and 5 a.m. local time and during geomagnetically quiet periods, following the selection criteria detailed in the WMM2025 Technical Report. The MF7 lithospheric field model (Maus et al., 2008) was removed from the Swarm data to exclude the static crustal field for spherical harmonic degrees 16 to 133. The CHAOS-8.4 model (Kloss et al., 2025) was applied to correct for magnetospheric field contributions. A series of 131 main field and secular variation models was then fitted to one-year data windows, spanning 2014.42 to 2025.33 at intervals of 1/12-year, using the method described in the WMM2025 Technical Report. Cubic smoothing splines were subsequently fitted to the main field model coefficients. The models used to assess the performance of the WMM and WMMHR models were extracted from these splines at the desired epochs. The splines for each coefficient were extrapolated to epoch 2026.0 using the spline time derivatives at epoch 2025.33.

Ground Observatory Data Processing

Root-mean-square-errors (RMSEs) between the WMM2020, WMM2025 and WMMHR2025 predicted secular variation (SV) and ground observatory data were calculated as follows. We took version 0146 (November 2025) of the auxiliary observatory data product (AUX_OBS_2) for 2020 to 2025, produced for the European Space Agency (ESA) Swarm mission. This contained selected definitive hourly means from the World Data Centre for Geomagnetism (Edinburgh) and hourly means provided as quasi-definitive (delivered soon after collection with manually checked baselines applied) by the International Real-time Magnetic Observatory Network (INTERMAGNET) or the observatory operator. Any reported steps due to observatory changes were applied. These data were provided by 120 observatories in 2020, 112 observatories in 2021, 101 observatories in 2022, 100 observatories in 2023, 82 observatories in 2024 and 60 observatories in 2025. We selected this data for geomagnetically quiet times when the Kp index was less than or equal to 2+, the rate of change of the Dst index was less than or equal to 5 nT/hour and the Bz component of Interplanetary Magnetic Field (IMF) was greater than or equal to −2 nT. We then selected only data from the hours of 1 a.m. to 2 a.m. local time. These conditions minimized contamination of the observations by external field sources to better reflect the background core field level that the WMM represents. The selected hourly data were averaged to monthly mean values, and then annual differences were taken to give SV values at the midpoint in time between a pair of samples at each observatory. Predictions of WMM2025 and WMMHR2025 SV were made at each time and location of an observation, and the RMSEs were calculated for each calendar year at each observatory, and for each calendar year globally.

The results presented in this report rely on data collected at magnetic observatories. We thank the World Data Centre (WDC) for Geomagnetism (Edinburgh; https://wdc.bgs.ac.uk), the national institutes that support observatories, and INTERMAGNET for promoting high standards of magnetic observatory practice (http://intermagnet.org).

Geomagnetic Virtual Observatory Data Processing

RMSEs between the WMM2025 and WMMHR2025 predicted SV and satellite virtual observatory data were calculated as follows. We took the monthly internal field SV estimates of the ESA Swarm Level 2 Geomagnetic Virtual Observatory data set version 0201 (September 2025), and calculated RMSEs relative to WMM2025 and WMMHR2025 using the same method as for the ground observatory data.

Magnetic Storms Data Processing

For each storm date listed in Table 5, we obtained seven days of minute mean values from global observatories on the INTERMAGNET website. This time window was centered on the peak day of the storm, or approximately to encompass storms with multiple peaks in activity. Using the best quality data available, viz definitive in preference to quasi-definitive in preference to provisional in preference to variation, seven-day means of declination were computed. If the data were not already in declination (D) angular units, easterly intensity (Y) and northerly intensity (X), both in nT units, were converted to D in angular units. For each storm and each observatory, a maximum absolute D deviation from the mean was then computed.